

# Friction Estimation and Compensation for Steering Angle Control for Highly Automated Driving

Marcus Walter, Norbert Nitzsche, Dirk Odenthal, Steffen Müller

**Abstract**—This contribution presents a friction estimator for industrial purposes which identifies Coulomb friction in a steering system. The estimator only needs a few, usually known, steering system parameters. Friction occurs on almost every mechanical system and has a negative influence on high-precision position control. This is demonstrated on a steering angle controller for highly automated driving. In this steering system the friction induces limit cycles which cause oscillating vehicle movement when the vehicle follows a given reference trajectory. When compensating the friction with the introduced estimator, limit cycles can be suppressed. This is demonstrated by measurements in a series vehicle.

**Keywords**—Friction estimation, friction compensation, steering system, lateral vehicle guidance.

## I. INTRODUCTION

**T**HE number of systems controlling the lateral vehicle dynamics increases rapidly. Parking manoeuvre and lane keeping assist can already be found in series production - others will follow. With an increasing number of lateral assistance systems the degree of automation grows. While current lane keeping systems merely support the driver, other approaches are emerging which take over the task of lane keeping autonomously.

The electric power steering, EPS, which is common in series vehicles, is the actuator usually used to guide the vehicle along its trajectory. A large number of different control concepts already exist. A structure for lateral vehicle guidance, described in [7] and [8], is used in this contribution. On the trajectory guidance level, the vehicle is controlled along the desired trajectory thereby rejecting external disturbances like crosswind. The output of the trajectory controller is a desired curvature which is input to the vehicle guidance controller, as a part of the vehicle guidance level. The curvature control is replaced with a steering angle control. Via the EPS actuator the desired steering angle is realized.

One of the challenges in steering angle control is dealing with various types of steering systems in different vehicles. The diversity of mechanic steering structures as well as occurring friction effects make a good control performance as well as zero steady state tracking more complex.

A high-precision position control of electromechanic systems is dealt with in many related papers across different fields like position control of robot joints [10], [9], or the moving

of nanometer machines [11]. Many position controllers compensate the friction by feedforward control which requires precise knowledge about friction between moving parts. Due to production tolerances, temperature and life cycle influences the friction in a steering system can vary significantly. Therefore, a constant feedforward compensation is not suitable for industrial applications. Adaptive friction compensation or observers can help but require parameter knowledge of the control plant. Especially in series vehicles it is difficult to determine the exact masses and stiffnesses of each part of the steering system.

This contribution introduces a zero steady state steering angle control for highly automated assistance systems, which observes the friction of the steering system with almost no knowledge of parameters. The controller takes the value of the observed friction into consideration and compensates it. The remainder of the paper is organized as follows: Section II gives an overview of friction models, compensation and observation. Section III presents the used control structure, including the steering angle controller, for highly autonomous driving. The friction estimator and compensation is introduced in section IV. The results of the friction estimation the improvement of the steering angle control due to friction compensation are shown in real world scenario, section V.

## II. FRICTION PHENOMENA AND ESTIMATION

Friction occurs in almost every moving mechanical system, where parts are in contact. The contribution [1] differentiates between "pre-sliding" and "sliding". According to the model in [1], the surface movement in pre-sliding range behaves like a nonlinear spring. Plastic movement occurs when this range is exceeded. In transition both elastic and plastic movement can be observed, which is the basis for the "bristle-model" [2]. For the sake of simplicity it is assumed that only one of the parts has bristles, which are randomly distributed on the surface, Fig. 1.

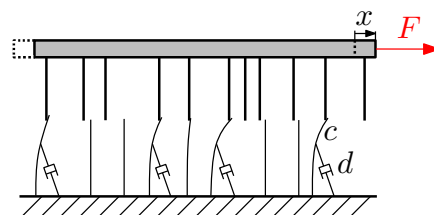


Fig. 1: Bristle model

Marcus Walter is with BMW AG, 80937 Munich, Germany (e-mail: Marcus.MA.Walter@bmw.de).

Norbert Nitzsche is with BMW AG, 80937 Munich, Germany (e-mail: Norbert.Nitzsche@bmw.de).

Dirk Odenthal is with BMW AG, 80937 Munich, Germany (e-mail: Dirk.Odenthal@bmw.de).

Steffen Müller is with Technical University of Berlin, 13355 Berlin, Germany (e-mail: Steffen.Mueller@tu-berlin.de).

Every bristle can be described as a spring-damper-element with values  $c$  and  $d$  and withstands a specific strain. Elastic-plastic movement  $x$  occurs when this specific strain  $F$  is exceeded. When all bristles lose contact the result is plastic movement.

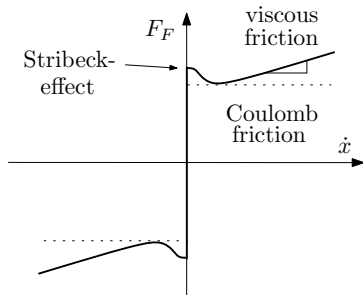


Fig. 2: Friction curve including Stribeck effect, viscous friction and Coulomb friction

Previously, Dahl developed a friction model based on stress-strain curve which describes the pre-sliding very accurately [3]. The behavior can be described with [4]:

$$\frac{dF}{dt} = \sigma v \left| 1 - \frac{F}{F_C} \operatorname{sgn}(v) \right|^i \left( 1 - \frac{F}{F_C} \operatorname{sgn}(v) \right), \quad (1)$$

with  $F_C$  as the value of the Coulomb friction and  $\sigma$  as a characteristic parameter. This model though does not take into consideration the Stribeck-effect at velocities around zero. The LuGre-model, presented in [5] and [6], improves this effect. This model takes different friction phenomena into consideration like pre-sliding displacement, frictional lag, varying break-away force and stick-slip motion.

Many papers which introduce feedforward friction compensation assume that friction is known in its shape and identified through previous measurements. This can be found in e.g. [12].

When the value of friction changes over operating time or is caused by production specific tolerances, a friction observer is necessary to determine changes. [14] introduces an observer on the assumption that only Coulomb friction appears and that the friction's value is the only parameter to be estimated. In the steering system which is subject of this work measurements have shown that stick-slip does not occur, but the existing viscous damping depends on the temperature and is therefore unknown. Hence, the approach described in [14] can not be applied to the problem in this contribution. [15] shows an adaptive friction compensation which observes friction including viscous damping. Applying this approach to the described problem, means that all external forces which act on the rack have to be known. The rack force caused by the tire side forces is difficult to determine due to the tires complexity and nonlinear behavior. Even though there are approaches for rack force observer like [13], they imply that the friction in the steering system is known in shape and value.

In summary, it can be said that common approaches of friction compensation assume that friction is previously identified

and friction models like (1) are parametrized. When they are unknown, parameter knowledge of masses and stiffnesses or external forces acting on the system are needed for friction observer.

At this point a very different observer for dry friction will be introduced which needs a few invariant parameters only. All required measurement signals can be measured with conventional sensors that are available in present vehicles.

### III. INFLUENCE OF FRICTION ON STEERING ANGLE CONTROL

This paper is dealing with friction estimation and compensation to improve the control performance of a steering angle controller for highly automated driving. This controller will be considered more closely in this section. The complete design of the controller and the control parameters can be found in [7], [8] and is not part of this contribution. Here, only the basic idea of the control structure, Fig. 3, is given which is necessary for understanding.

The trajectory tracking control, TTC, tracks the reference

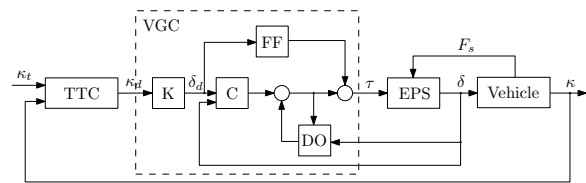


Fig. 3: Control structure with trajectory tracking control TTC and vehicle guidance control VGC

value  $\kappa_t$ , e.g. the centerline of a road with  $\kappa_d$  as input to the VGC.  $K$  converts the curvature  $\kappa_d$  to a desired steering angle  $\delta_d$ , based on an inverse model of the vehicle. The steering angle control is performed by controller,  $C$ , supported by the feedforward control,  $FF$ . To suppress steering angle disturbances caused by e.g. uneven roads and to guarantee steady state accuracy, a disturbance observer,  $DO$ , is used, which shows an integrating behavior [8]. The control signal  $\tau = \tau_{VGC}$  is output of the VGC and acts on the EPS which leads to rack travel, so that the vehicle follows the desired trajectory  $\kappa_t$ .

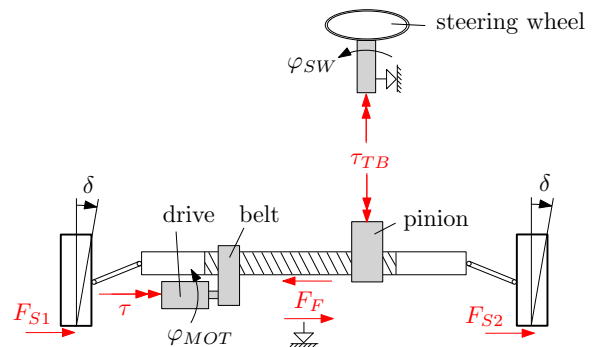


Fig. 4: Two-mass EPS system with friction reduced to the rack

Fig. 4 shows a two degrees of freedom model of the steering system. The tire side forces  $F_{S1} + F_{S2} = F_S$  act on the rack with transmission ratio  $i_S$  of tie rod, steering arm and pneumatic and kinematic trail. Friction occurs in various parts, especially at bearings, belt and pinion which connects torsion bar and rack. Measurements on a test rack did not show a Stribeck-effect. The VGC shows robust performance against varying viscous friction, which means, that the exact value must not be known. The impact of the Coulomb friction is more critical for high precision control.

Considering the "lower" part of the steering system, including pinion, EPS, rack and wheels, (Fig. 4), the friction of all subcomponents can be reduced to one friction, which acts on the rack. Unless otherwise indicated, the term "friction" refers to Coulomb friction and is depicted as  $F_F$ . By means of the belt's transmission ratio  $i_{EPS}$ ,  $F_F$  can be converted to the EPS:

$$\tau_F = F_F \frac{1}{i_{EPS}}. \quad (2)$$

The control signal  $\tau$  must exceed the Coulomb friction  $F_F$ , before the rack starts to move, Fig. 5. This results in limit cycles which are transferred to the yaw dynamics of the vehicle. Hence, the vehicle makes an oscillating movement.

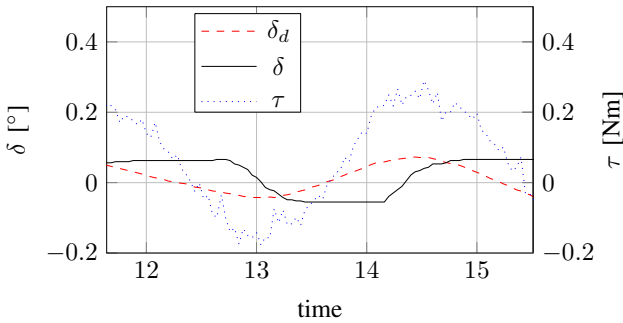


Fig. 5: Sticking of the steering system angle  $\delta$

By increasing the integrating behaviour of  $DO$ , the effect of limit cycles could be deteriorated. However, the transfer behavior from  $\delta_d$  to  $\delta$  would get worse since the rejection of measurement noise decreases. Friction compensation in the outer cascade TTC is dynamically too slow and does not work either.

For these reasons, a friction compensation is needed to suppress the limit cycles. To do this, an estimation is introduced to determine the friction with respect to industrial purposes.

#### IV. FRICTION ESTIMATION AND COMPENSATION

##### A. Friction Estimation

Considering the steering system cut off from the steering wheel and road, the torsion bar torque  $\tau_{TB}$ , the EPS torque  $\tau_{EPS}$ , the tire force  $F_S$  and the friction force  $F_F$  act on the system. Assuming very small steering angle velocities  $\dot{\delta}_{min} < |\dot{\delta}| < \dot{\delta}_{max}$  with  $\dot{\delta}_{min}, \dot{\delta}_{max} > 0$ , the inertia force

can be neglected and the following formula applies:

$$\tau_{TB} i_{TB} + \tau_{EPS} i_{EPS} = F_S i_S + F_F \quad \text{resp.} \quad (3)$$

$$F_{TB} + F_{EPS} = F_{S,RK} + F_F, \quad (4)$$

with  $i_{TB}$ ,  $i_{EPS}$  and  $i_S$  being the transmission ratios of the rack, which are usually known. The EPS torque  $\tau_{EPS}$  as well as the torsion bar torque  $\tau_{TB}$  are measurable. The ratios  $i_{TB}$ ,  $i_{EPS}$  and  $i_S$  are known. Plotting the sum  $F_{TB} + F_{EPS} = F_{SUM}$  against the steering angle  $\delta$ , one gets the friction hysteresis shown in Fig. 6. The difference between the positive and negative zero crossing is twice the value of the Coulomb friction, means  $2F_F$ . For the sake of clarity,  $F_F$  denotes the measured value.

The more measurement values can be evaluated, the more precise the result is. Hence, the considered steering angle range is defined from  $-\delta_{max}$  to  $\delta_{max}$ . This range gets divided into  $n$  pair of clusters  $\Delta_1^{+/-} \dots \Delta_n^{+/-}$ . The friction value is determined in every cluster, respectively. Afterwards, the average is taken over all friction values of each of the  $n$  clusters.

The indices and conventions for the following mathematical calculations are as follows:

$$i \in [1, n] \quad \text{Number of cluster,} \quad (5)$$

$$k \in [1, p] \quad \text{Number of measurement points.} \quad (6)$$

Depending on the sign of the steering angle velocity  $\dot{\delta}$  the measurement values  $F_{TB,k} + F_{EPS,k} = F_{F,k}$  are assigned to a positive cluster  $\Delta_i^+$  or a negative cluster  $\Delta_i^-$ :

$$F_{F,k} \rightarrow \Delta_1^+ \quad | \quad \delta_k \in [\delta_1, \delta_2[ \cap \dot{\delta}_k \in [\dot{\delta}_{min}, \dot{\delta}_{max}]$$

$$F_{F,k} \rightarrow \Delta_1^- \quad | \quad \delta_k \in [\delta_1, \delta_2[ \cap \dot{\delta}_k \in [-\dot{\delta}_{max}, -\dot{\delta}_{min}]$$

$$F_{F,k} \rightarrow \Delta_2^+ \quad | \quad \delta_k \in [\delta_2, \delta_3[ \cap \dot{\delta}_k \in [\dot{\delta}_{min}, \dot{\delta}_{max}]$$

$$\vdots$$

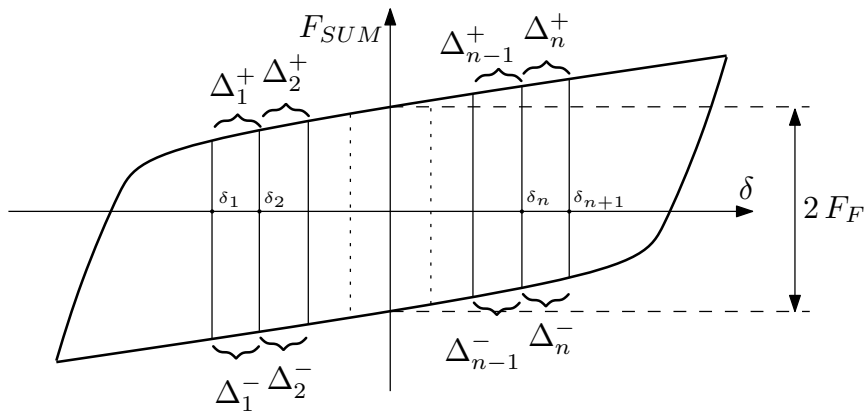
$$\vdots$$

$$F_{F,k} \rightarrow \Delta_n^- \quad | \quad \delta_k \in [\delta_n, \delta_{n+1}[ \cap \dot{\delta}_k \in [-\dot{\delta}_{max}, -\dot{\delta}_{min}].$$

If two paired clusters ( $\Delta_i^-$  and  $\Delta_i^+$ ) contain more than one measurement value, the average of these clusters is taken, which results in the friction  $F_{F,i}$ . Finally, the mean value of all  $n$  single averages is the friction  $F_F^*$ :

$$F_F^* = \frac{1}{n} \sum F_{F,i} \quad , \quad i \in [1, n]. \quad (7)$$

Because of lateral road inclination the hysteresis can be moved in vertical direction. Hence, it makes sense that the measurement values are subject to ageing. An ageing over time is inadequate, since the vehicle covers a long distance when driving with high speed, whereby the road condition can strongly change. For this reason an ageing over distance is introduced, by means of the velocity-dependent time constant  $T(v)$ . This is calculated for each cluster individually:


 Fig. 6: Friction hysteresis with clusters  $\Delta_1^{+/-}$ 

$$F_{F,i,k} = \frac{F_{F,k}}{1 + \frac{T(v)}{T_s}} + \frac{F_{F,i,k-1}}{1 + \frac{T_s}{T(v)}}, \quad (8)$$

with  $T_s$  as the sample time. The higher the velocity, the faster the measurement values age.

### B. Friction Compensation

Structures for friction compensation can be found in [1], [6]. Here, a feedforward compensation depending on the control error  $e = \delta_d - \delta$  is used. The compensation torque  $\tau_{F,c}$  is added to input  $\tau_{VGC}$ , as shown in Fig. 7:

$$\tau = \tau_{VGC} + \tau_{F,c} \quad (9)$$

with

$$\tau_{F,c} = \begin{cases} F_F^*/i_{EPS} & \text{if } e > e_{TZ} \\ -F_F^*/i_{EPS} & \text{if } e < -e_{TZ} \\ 0 & \text{if } -e_{TZ} \leq e \leq e_{TZ} \end{cases} \quad (10)$$

with  $e_{TZ} > 0$  as a small control error, which prevents the compensation torque from oscillating.

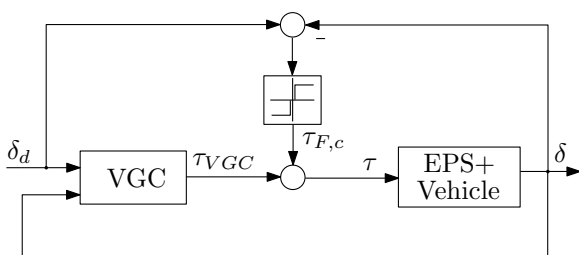


Fig. 7: Control structure with friction compensation

## V. RESULTS

The friction estimator as well as the TTC and VGC were implemented in a test vehicle. The estimation and control performance were tested in real world scenarios.

The value of friction which was measured on a test rack is assumed to be 100%. One can see, that the estimated friction fits very well to the reference value, Fig. 8. The initial value

for the estimator is  $\sim 50\%$ . After 100s the estimated value converges towards the measured.

Choosing  $F_c$  to 100% to compensate the friction, the amplitude and frequency of the limit cycle decreased significantly, Fig. 9 and Fig. 10. The control activity to keep the vehicle on track are not perceptible in yaw dynamics for human. The results demonstrate that the friction estimator is well suited for industrial purposes.

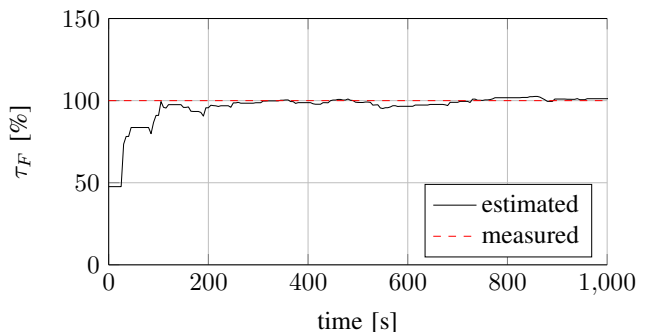
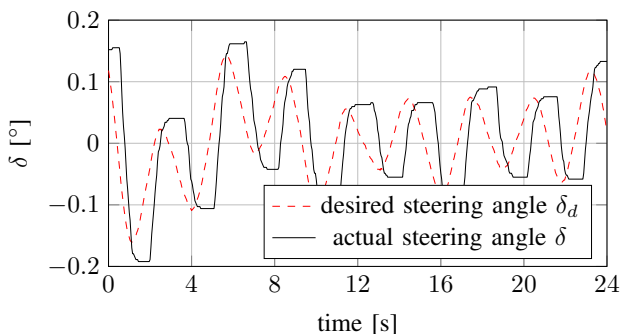

 Fig. 8: Observed friction with initial value of  $\sim 50\%$ 


Fig. 9: Lane keeping without friction compensation

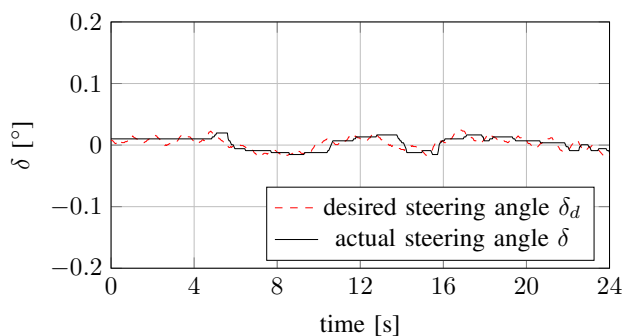


Fig. 10: Lane keeping with friction compensation

The best control performance can be achieved, when the real friction value is known exactly and is estimated in a very short time. However, this is difficult to achieve. The effects of undercompensation and overcompensation of friction are investigated in [16]. It was established, that undercompensation is favoured over overcompensation since the latter increases the amplitude of the limit cycles. This effect was also established in these investigations. Therefore it is appropriate to compensate the observed friction only to a part to be robust against errors of observation and to avoid overcompensation.

## VI. CONCLUSIONS

In this contribution a friction estimator for industrial purpose which identifies Coulomb friction in a steering system was presented. Determination of parameters like masses and stiffnesses in series cars, can only be done with a high effort. For this reason the presented estimator only needs parameters which are usually known and time invariant. All measurement signals can be captured with sensors that are available in every series vehicle. The friction estimator works only under certain conditions - small steering angles as well as small steering angle velocities. By means of the torsion bar torque and the EPS torque the friction hysteresis was calculated. A control structure for lateral vehicle guidance was introduced. A desired trajectory, e.g. the centerline of a road, is reference value for the trajectory tracking control. The subordinate vehicle guidance controller, with the motor torque as an input to the EPS, performs a steering angle control so that the vehicle follows the reference line. The friction in the steering system induces limit cycles which causes oscillating vehicle movement. When compensating the estimated friction, limit cycles can be suppressed.

## REFERENCES

- [1] B. Armstrong-Hélouvy, P. Dupont and C.C. de Wit, *A survey of models, analysis tools and compensation methods for the control of machines with friction*, *Automatica* 30.7: 1083-1138, 1994
- [2] D.A. Haessig, B. Friedland, *On the modeling and simulation of friction*, *Journal of Dynamic Systems, Measurement, and Control*, 113(3), 354-362, 1991
- [3] P.R. Dahl, *A solid friction model* (No. TOR-0158 (3107-18)-1). AEROSPACE CORP EL SEGUNDO CA, 1968
- [4] P.R. Dahl, *Solid friction damping of spacecraft oscillations* (No. TR-0076 (6901-03)-2). AEROSPACE CORP EL SEGUNDO CALIF GUIDANCE AND CONTROL DIV, 1975

- [5] C.C. de Wit, H. Olsson, K.J. Åström, and P. Lischinsky, *A new model for control of systems with friction*, *Automatic Control, IEEE Transactions on*, 40(3), 419-425, 1995
- [6] H. Olsson, K.J. Åström, C.C. de Wit, M. Gäfvert, P. Lischinsky, *Friction models and friction compensation*, *European journal of control*, 4(3), 176-195, 1998
- [7] C. Rathgeber, F. Winkler, D. Odenthal and S. Müller, *Lateral trajectory tracking control for autonomous vehicles*, In *European Control Conference (ECC)*, 1024-1029, 2014
- [8] M. Walter, N. Nitzsche, D. Odenthal and S. Müller, *Lateral vehicle guidance control for autonomous and cooperative driving*, In *European Control Conference (ECC)*, 2667-2672, 2014
- [9] L. Le Tien, A. Albu-Schäffer, A. De Luca and G. Hirzinger, *Friction observer and compensation for control of robots with joint torque measurement*, *IEEE/RSJ International Conference on Intelligent Robots and Systems*, 3789-3795, 2008
- [10] P. Lischinsky, C.C. de Wit and G. Morel, *Friction compensation for an industrial hydraulic robot*, *Control Systems, IEEE*, 19(1), 25-32, 1999
- [11] A. Amthor, T. Hausotte, C. Ament, P. Li and G. Jäger, *Friction identification and compensation on nanometer scale*, In *Proc. IFAC World Congress* (pp. 2014-2019), 2008
- [12] L. Márton and B. Lantos, *Modeling, identification, and compensation of stick-slip friction* *Industrial Electronics, IEEE Transactions on*, 54(1), 511-521, 2007
- [13] S.A. Fankem, T. Weiskircher and S. Müller, *Model-Based Rack Force Estimation for Electric Power Steering* In *World Congress* (Vol. 19, No. 1, pp. 8469-8474), 2014
- [14] J. Amin, B. Friedland and A. Harnoy, *Implementation of a friction estimation and compensation technique* *Control Systems, IEEE*, 17(4), 71-76, 1997
- [15] B. Friedland and Y.J. Park, *On adaptive friction compensation* *Automatic Control, IEEE Transactions on*, 37(10), 1609-1612, 1992
- [16] D. Putra, H. Nijmeijer and N. van de Wouw, *Analysis of undercompensation and overcompensation of friction in 1DOF mechanical systems* *Automatica*, 43(8), 1387-1394, 2007